

Inscription of Bragg gratings in few-mode optical fibers

Peng Guo (郭 鹏)¹, Yunjiang Rao (饶云江)^{1*}, Dengyong Li (李登勇)¹, Yuan Gong (龚 元)¹,
Gangding Peng², Yu Wu (吴 宇)¹, Weili Zhang (张伟利)¹, and Huijuan Wu (吴慧娟)¹

¹Key Lab of Optical Fiber Sensing and Communications (Education Ministry of China),
University of Electronic Science and Technology of China, Chengdu 611731, China

²School of Electrical Engineering and Telecommunications, University of New South Wales, Sydney, NSW 2052, Australia

*Corresponding author: yjrao@uestc.edu.cn

Received July 10, 2012; accepted October 10, 2012; posted online January 21, 2013

Few-mode fiber Bragg grating (FM-FBG) has wide applications in the field of multi-wavelength fiber lasers and fiber-optic sensing. In this letter, FBG is successfully written in a novel type of FM fiber (FMF) based on 248-nm excimer laser and a uniform phase mask. A low-loss coupling between the FMF to a single-mode fiber is realized by a graded-index multi-mode fiber with a length of about a quarter pitch. The sensing properties of the FMF grating are further investigated. The experimental results indicate that the novel FM-FBG has sensitivities of temperature, strain, and bending of 11.2 pm/°C, 1.3 pm/μ ϵ , and 636.9 pm/m⁻¹, respectively.

OCIS codes: 060.2370, 060.3735.

doi: 10.3788/COL201311.020606.

Since Hill *et al.* fabricated the fiber Bragg grating (FBG) in the fiber^[1] for the first time using the phase mask method, the FBG has been widely used in optical fiber communication and sensing^[2–6]. The fiber gratings are usually written in single-mode fiber (SMF) by interference method or a phase mask technique, and its characteristics have been extensively investigated. Given that FBGs in the multi-mode fiber (MMF) or few-mode fiber (FMF) have special spectral characteristics^[7,8], they have found novel applications in the field fiber laser^[9,10] and fiber-optic interferometer. The characteristics and applications of FBGs in the MMF or FMF have been investigated in previous works^[11–13]. However, in these FBGs, the low loss coupling between optical fibers with different mode field diameters must be carefully considered^[14].

In this letter, FBGs are inscribed in a novel FMF by employing the standard inscription method. The refractive index distribution of the novel FMF has been described in Ref. [15]. The 3D light intensity distribution from the optical fiber end, with a length of 72 mm FMF fusion spliced to the lead-in SMF (Fig. 1). A novel fiber structure based on a short section of graded-index MMF (GI-MMF) is developed in order to obtain the low loss coupling between the FMF and SMF. The core diameters of SMF, FMF, and GI-MMF are 8.9, 15.0, and 62.5 μm, respectively. The experiments show that this structure can greatly reduce the coupling loss of the reflection peak of the higher-order modes of few-mode FBG (FM-FBG). The temperature, strain, and bending responses of the FM-FBG are also experimentally investigated.

Light is periodically focused and diverged along the GI-MMF due to the parabolic refractive index distributions of GI-MMF in the radial direction. In this experiment, a section of GI-MMF with a length of a quarter pitch was selected in order to converge the light transmitted or reflected from the FMF into the SMF, which led into the optical spectrum analyzer (OSA).

An OSA (MS9710C, Anritsu, Japan) integrated with a broadband light source (86142A, Hewlett-Packard, USA)

for calibration was used to investigate the coupling loss of three fiber structures (Fig. 2). In the first one, the light was transmitted directly through a standard SMF (Fig. 2(a)). The average transmitted intensity was set as reference to about -49.12 dBm (Fig. 3). In the second, a section of FMF with length of 200 cm was fusion spliced between SMFs (Fig. 2(b)). The average transmitted intensity was about -54.29 dBm, corresponding to a total

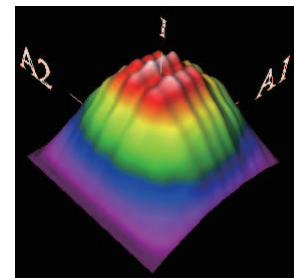


Fig. 1. Light intensity distribution from the FMF end.

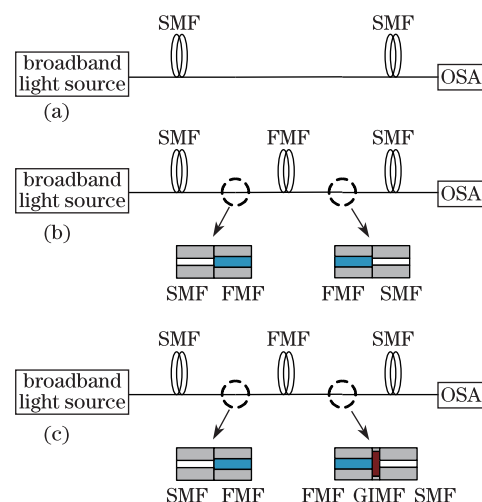


Fig. 2. Three fiber-optic structures in the coupling experiments.

loss of 5.17 dBm. The total loss included the coupling loss at the FMF-SMF joint and the transmission loss of the FMF. In the third, a short section of GI-MMF with a length of about a quarter pitch (0.52 mm) was fusion spliced between the FMF and the SMF at the output end of the FMF (Fig. 2(c)). The coupling loss was 0.79 dBm, and was reduced by 4.38 dBm compared with the second structure.

The FMF fiber was exposed to high-pressure hydrogen at 12 MPa and 70 °C for 2 days to increase its photosensitivity. Then, the FMF was exposed to the ultraviolet (UV) laser pulses behind the uniform phase mask, as shown in the experimental setup in Fig. 4. The UV pulses were provided by a KrF excimer laser (BraggStar Industrial-1 000-248 nm-FT, Coherent, Inc.). Laser output energy of 6.30 mJ and a repetition rate of 100 Hz were chosen. A total of 300 laser pulses were used for the FM-FBG inscription. We roughly optimized the laser energy and the exposure time by manufacturing 10 FM-FBGs under different parameters, after which we chose the best one for use in the sensing experiments.

The period of phase mask was set to 1070.5 nm, and the corresponding period of FBG was set to half of the phase mask period (535.25 nm). The center wavelength of the FMF fundamental mode reflection peak was 1554.336 nm in the experiment. The Bragg condition is given as

$$\lambda = 2\bar{n}\Lambda, \quad (1)$$

where λ is the center wavelength of the FBG, \bar{n} is the refractive index of the fiber core, and Λ is the period of FBG. Thus, the effective index of the FMF calculated from the Bragg wavelength is 1.452.

The reflective spectrum of the FM-FBG, coupled directly back to the lead-in SMF is shown in Fig. 5(a). In the reflective spectrum of FM-FBG, there are 3 Bragg

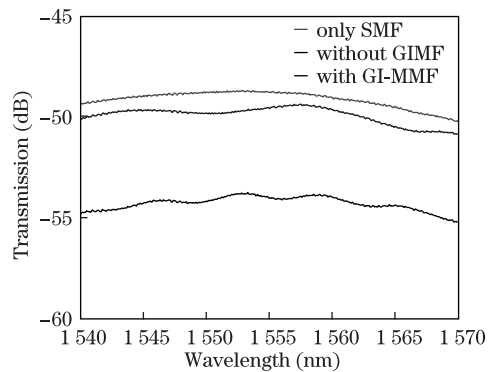


Fig. 3. Transmission spectra of the three fiber-optic structures.

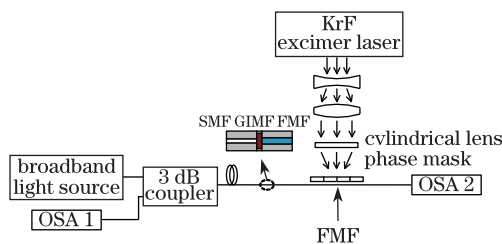


Fig. 4. Schematic diagram of the experimental setup for the inscription of the FBG in the FMF.

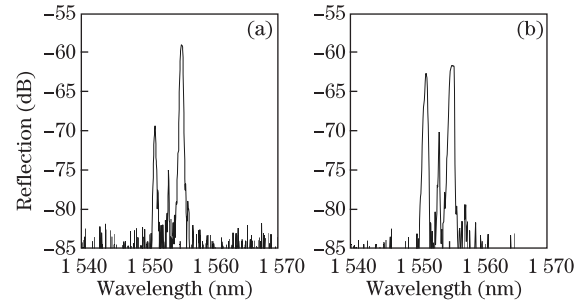


Fig. 5. Reflective spectra of the FM-FBG (a) coupled directly back to the lead-in SMF and (b) coupled to the SMF via a short section of GI-MMF.

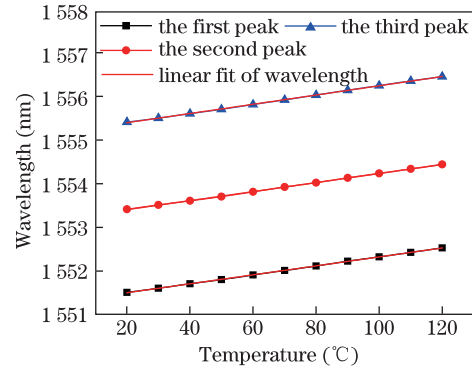


Fig. 6. Temperature responses of the FM-FBG.

peaks of around 1550 nm. The number of modes excited in FMF determines the multi-peak structure in the reflective spectrum. From left to right, the Bragg peaks respectively correspond to the LP₁₁, LP₂₁, and LP₀₁ modes. Using the GI-MMF coupling device, the reflections of the Bragg peaks for the LP₁₁ and LP₂₁ modes increase by 6.7 and 4.9 dB, respectively (Fig. 5(b)). The maximum reflectivity of the FM-FBG is greater than 92%.

In order to improve the sensing performance, an optical sensing interrogator (Model Si425, Micron Optics Inc., USA) was employed in this letter instead of the OSA. The wavelength repeatability is found to be better than 0.2 pm, and the typical wavelength stability is about 2 pm. The FM-FBG sample was tested for temperature response in the temperature cycling bins (LP150A, Hongzhan, China), with initial temperature of 20 °C. This initial temperature increases up to 120 °C with a step of 10 °C. The experimental result is shown in Fig. 6. The temperature sensitivity of the 3 peaks are 11.0, 10.9 and 11.2 pm/°C, respectively. The linearity is better than 99.9%.

The strain response of the FM-FBG was tested. Both the fiber ends were fixed using home-made fiber clamps on two adjustable stages with a spatial resolution of 10 μm; the ends were separated at a distance of 100 cm. The experimental results are shown in Fig. 7. The strain sensitivities of the 3 wavelength peaks are almost the same at 1.3 pm/μ ϵ ; in addition, the linearities of all three curves are higher than 99.9%.

The experimental setup used for testing the bending responses is similar to that used in Ref. [16]. The FM-FBG under the metal beam was set in the center of two clamps, and the distance between the edges of the two

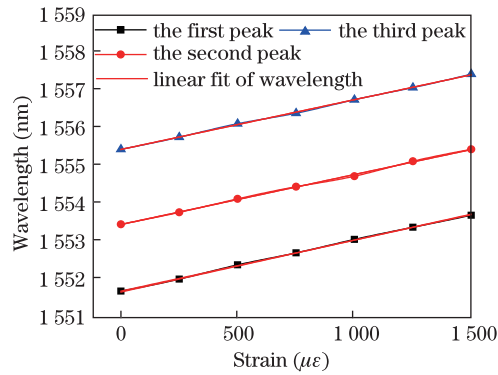


Fig. 7. Strain responses of the FM-FBG.

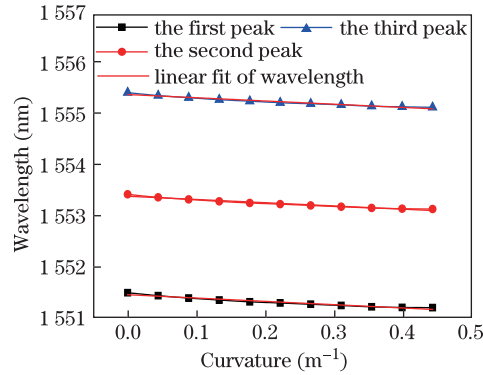


Fig. 8. Bending responses of the FM-FBG.

clamps was represented by L . The bending displacement d was adjusted by pressing the center of the metal beam with a vertically-adjustable stage. In this way, the fiber structure bent freely and synchronously with the metal beam. The curvature of the FM-FBG could be determined by $\rho = 2d/(d^2 + L^2)^{1/2}$ ^[16]. The result is shown in Fig. 8. Variations of the center wavelengths of the 3 peaks of the curvature are -654.1 , -638.2 , and -636.9 pm/m⁻¹, respectively. The linearities of all three curves are higher than 99.5%.

In conclusion, FBGs are inscribed in a novel FMF based on the 248-nm excimer laser and a uniform phase mask. The coupling losses between the FMF and a standard SMF are greatly reduced by inserting a short section of the GI-MMF. The sensing properties of the FM-FBG are fully explored, and we hope this kind of novel FBG can find applications in the field of sensing or multi-wavelength lasers.

This work was supported by the National Natural Science Foundation of China (Nos. 61107073, 61107072, and 61106045), the Fundamental Research Funds for the Central Universities of China (No. ZYGX2011J002), the Research Fund for the Doctoral Program of Higher Education of China (No. 20110185120020), and the Open Research Fund of State Key Laboratory of Transient Optics and Photonics, Chinese Academy of Sciences (No. SKLST201005).

References

1. K. O. Hill, B. Malo, F. Bilodeau, D. C. Johnson, and J. Albert, *Appl. Phys. Lett.* **62**, 1035 (1993).
2. A. D. Kersey, M. A. Davis, H. J. Patrick, M. LeBlanc, K. P. Koo, C. G. Askins, M. A. Putnam, and E. J. Friebele, *J. Lightwave Technol.* **15**, 1442 (1997).
3. X. Y. Dong, H. Zhang, B. Liu, and Y. P. Miao, *Photon. Sens.* **1**, 6 (2011).
4. A. P. Zhang, S. R. Gao, G. F. Yan, and Y. B. Bai, *Photon. Sens.* **2**, 1 (2012).
5. B. Guan, H. Y. Tam, X. M. Tao, and X. Y. Dong, *IEEE Photon. Technol. Lett.* **12**, 675 (2000).
6. L. Yu, J. Lit, X. J. Gu, and L. Wei, *Opt. Express* **13**, 8508 (2005).
7. T. Mizunami, T. V. Djambova, T. Niiho, and S. Gupta, *J. Lightwave Technol.* **18**, 230 (2000).
8. W. W. Morey, G. Meltz, J. D. Love, and S. J. Hewlett, *Electron. Lett.* **30**, 730 (1994).
9. X. H. Feng, Y. Liu, S. G. Fu, S. Z. Yuan, and X. Y. Dong, *IEEE Photon. Technol. Lett.* **16**, 762 (2004).
10. D. S. Moon, U. C. Paek, and Y. J. Chung, *Opt. Express* **12**, 6147 (2004).
11. Y. G. Han, S. B. Lee, D. S. Moon, and Y. J. Chung, *Opt. Lett.* **30**, 2200 (2005).
12. A. Stefani, W. Yuan, C. Markos, and O. Bang, *IEEE Photon. Technol. Lett.* **23**, 660 (2011).
13. C. L. Zhao, X. F. Yang, M. S. Demokan, and W. Jin, *J. Lightwave Technol.* **24**, 879 (2006).
14. A. Mafi, P. Hofmann, C. J. Salvin, and A. Schülzgen, *Opt. Lett.* **36**, 3596 (2011).
15. N. Bai, E. Ip, Y. K. Huang, E. Mateo, F. Yaman, M. J. Li, S. Bickham, S. Ten, J. Liñares, C. Montero, V. Moreno, X. Prieto, V. Tse, K. M. Chung, A. P. T. Lau, H. Y. Tam, C. Lu, Y. H. Luo, G. D. Peng, G. F. Li, and T. Wang, *Opt. Express* **20**, 2668 (2012).
16. Y. Gong, T. Zhao, Y. J. Rao, and Y. Wu, *IEEE Photon. Technol. Lett.* **23**, 679 (2011).